

Comparison of next-generation sequencing quality metrics and concordance in the detection of cancer-specific molecular alterations between formalin-fixed paraffin-embedded and fresh-frozen samples in comprehensive genomic profiling with the Illumina® TruSight Oncology 500 assay

DUŠAN LODERER¹, ANDREA HORNÁKOVÁ¹, KATARÍNA TOBIÁŠOVÁ², KATARÍNA LEŠKOVÁ², ERIKA HALAŠOVÁ¹, ZUZANA DANKOVÁ^{1,3}, KAMIL BIRINGER⁴, ERIK KÚDELA⁴, TOMÁŠ ROKOS⁴, ANTON DZIAN⁵, JURAJ MIKLUŠICA⁶, PETER MIKOLAJČÍK⁶, MAREK SMOLÁR⁶, LUKÁŠ PLANK² and MARIÁN GRENDÁR¹

¹Biomedical Centre Martin, Jessenius Faculty of Medicine in Martin, Comenius University Bratislava, 036 01 Martin, Slovakia;

²Department of Pathological Anatomy, Jessenius Faculty of Medicine in Martin, Comenius University Bratislava and University Hospital in Martin, 036 01 Martin, Slovakia; ³Biobank for Cancer and Rare Diseases, Jessenius Faculty of Medicine in Martin, Comenius University Bratislava, 036 01 Martin, Slovakia; ⁴Clinic of Obstetrics and Gynaecology, Jessenius Faculty of Medicine in Martin, Comenius University Bratislava, 036 01 Martin, Slovakia; ⁵Department of Thoracic Surgery, Jessenius Faculty of Medicine in Martin, Comenius University Bratislava, 036 59 Martin, Slovakia; ⁶Clinic of General, Visceral and Transplant Surgery, Jessenius Faculty of Medicine in Martin, Comenius University Bratislava, 036 59 Martin, Slovakia

Received November 4, 2024; Accepted December 19, 2024

DOI: 10.3892/etm.2025.12814

Abstract. Next-generation sequencing (NGS) technology is routinely employed to detect clinically significant variants in the field of precision medicine. Formalin-fixed paraffin-embedded (FFPE) tissues remain a widely used source of genetic material for diagnostic purposes due to their long-term storage stability, which preserves the architecture of tumour tissues. However, the degradation of nucleic acids (NAs) that occurs during the fixation process can lead to unreliable results or hinder analysis. Considering the challenges posed by the quality and quantity of nucleic acids extracted from FFPE samples, the present study aimed to compare paired fresh-frozen (FF) and FFPE samples. The present study also aimed to assess the concordance rate of quality control metrics of sequenced libraries and identify variants and biomarkers between FFPE and FF tissues. The

Illumina® TruSight Oncology 500 assay (TSO 500; Illumina, Inc.) was used to conduct comprehensive genomic profiling of samples from patients with various cancer types. All identified alterations were annotated using the Pierian Dx Clinical Genomics Workspace version 6.20 (PierianDx CGW). A total of 138 DNA and 138 RNA analyses on 69 paired samples were performed. These results demonstrated the significant potential of FF tissue as a primary source of higher-quality genetic material to detect small variants, microsatellite instabilities and the tumour mutational burden, using the TSO 500 assay compared with FFPE samples. This approach could effectively reduce the issues associated with poor-quality NAs extracted from FFPE samples. Based on our findings of lower concordance in the detection of splice variants, fusions and copy number variants in paired samples, we recommend that future studies using the TSO 500 assay should focus directly on this issue.

Correspondence to: Dr Andrea Hornáková, Biomedical Centre Martin, Jessenius Faculty of Medicine in Martin, Comenius University Bratislava, Malá Hora 4C, 036 01 Martin, Slovakia
E-mail: andrea.hornakova@uniba.sk

Key words: next generation sequencing, Illumina® TruSight Oncology 500 assay, PierianDx Clinical Genomics Workspace, quality metrics, concordance, formalin-fixed paraffin-embedded tissue, fresh-frozen tissue

Introduction

Precise, rapid and comprehensive diagnostics are key to the effective selection of available procedures and medications that can significantly improve the quality of life of patients with cancer. The widespread use of next-generation sequencing (NGS) technology, which allows for rapid and precise identification of cancer-specific alterations in a broad range of genes, has refined this branch of diagnostics and increase the use of personalized therapies. Based on the available information, clinically relevant molecular alterations can be divided into

the following groups: Small variants, including single-nucleotide variants (SNVs; insertions and deletions), splice variants, fusions and copy number variants (CNVs). An integral part of the diagnostic process is also the determination of genomic biomarkers such as microsatellite instability (MSI) and tumour mutational burden (TMB). The TruSight Oncology 500 (TSO 500; Illumina, Inc.) assay can be used to analyse small variants in 523 tumour-associated genes, detection of three types of clinically relevant splice variants, identification of the presence of fusions in 55 selected genes, CNV analysis of 59 genes and TMB and MSI detection in formalin-fixed paraffin-embedded (FFPE) samples (1-3). Along with the possibility of annotating identified changes using software such as PierianDx CGW (Pierian), this type of comprehensive assay represents a unique solution for diagnosing a wide range of oncological diseases. However, a complex analysis requires a sufficient quantity and quality of extracted nucleic acids. Since FFPE samples currently remain the most used type of material in the diagnostic process, the TSO 500 assay is also primarily intended for use with FFPE samples (1-6).

The performance of the TSO 500 assay using FFPE samples has been evaluated by multiple studies that have obtained comparable results (1-5). These findings support the rationale for utilising this type of test for comprehensive genomic profiling across various tumour types (1-6). However, the aspect of feasibility of analysis should be considered. It is not uncommon for the low quality of nucleic acids to preclude the analysis of a relatively high percentage of FFPE samples, whether by classic methods such as fluorescence *in situ* hybridisation and immunohistochemistry or by NGS-based assays (7-10). One way to avoid repeated and potentially unsuccessful attempts at extracting nucleic acids from low-quality FFPE samples is to use non-FFPE material.

Several scientific studies have focused on determining the performance of NGS using non-FFPE material. However, these studies could not assess the concordance of NGS quality metrics and performance in detecting alterations of FFPE vs. non-FFPE tissues due to the absence of paired samples (6,11).

The present study aimed to focus on comparing the quality control (QC) parameters as well as the concordance of variant detection methods between findings from FFPE and fresh-frozen (FF) samples in the detection of clinically relevant gene alterations identified by the TSO500 assay and annotated using PierianDx CGW. Paired samples of lung carcinoma of non-small cell type (LC), breast carcinoma (BC) and colorectal carcinoma (CRC) that met the required quality criteria were analysed.

Materials and methods

Sample collection. The specimens used in the present study were prospectively collected to allow complex genomic profiling of the tumour and tumour-adjacent tissues of patients with LC, BC and CRC in paired FFPE and FF tissue samples. All patients provided written informed consent for participation in the study and the study was approved by the Ethics Committee of the Jessenius Faculty of Medicine in Martin (approval no. EK 79/2020; Martin, Slovakia). Patient tissue samples were collected between January 2021 and March 2022 at the University Hospital Martin (Martin, Slovakia).

The standard operation protocols used at the hospital for each type of surgical specimen were adapted to ensure routine standard diagnostic procedures were performed, whilst allowing all tissues required to be collected for the present study. As the surgical department was located close to the pathology laboratories, it was possible to deliver the unfixed resected specimen to the gross pathology laboratory immediately after completing the surgical examination.

Processing and storage of FFPE and FF samples. The responsible pathologists, while reviewing the delivered unfixed specimens to ensure the required routine diagnostic procedures, selected the samples to be stored in a FF state. The tumour tissue had to be of sufficient volume to make two aliquots. Of these aliquots, one was intended for fixation, and the other, with a volume of $\sim 3.4 \text{ mm}^3$, was used for the extraction of nucleic acids and was submerged in a volume of RNeasy Protect Tissue Reagent (Qiagen GmbH) and banked in ultra-low temperature freezers at -80°C at the Biomedical Centre Martin (Martin, Slovakia). After standard formalin fixation and grossing of the specimen, where samples were fixed in 10% neutral buffered formalin (pH 7.2-7.4; formaldehyde 4%) (cat. no. 02170107; BD Bamed s.r.o) at 25°C for 24 h, the parallel tissue samples were embedded in paraffin wax together with all the tissue samples required for routine oncological biopsy diagnostics. For the present study, prior to the extraction of DNA and RNA, FFPE blocks were selected and $20 \mu\text{m}$ paraffin sections were prepared using a microtome (Microm HM 400; Zeiss GmbH). The first section(s) were dedicated to nucleic acid extraction, while the subsequent section was stained with haematoxylin and eosin to enable the responsible pathologist to determine the tumour:cell ratio. All FFPE samples were stored under standardized conditions, with a median age of 17 months, ranging from 9-25 months. Only samples with a sufficient volume and $>20\%$ tumour cells (TCs) were accepted. Although direct quantification of the tumour:cell ratio for the FF samples was not performed, the FF and FFPE tissues originated from adjacent parallel sections. Therefore, it was assumed that the TC ratio was likely to be similar.

Nucleic acid extraction and quality assessment of FFPE samples. For simultaneous DNA and RNA extraction, a total of four $20 \mu\text{m}$ sections of FFPE tissue were assayed using the AllPrep[®] DNA/RNA FFPE kit (cat. no. 80234; Qiagen GmbH), according to the manufacturer's instructions. For a gentler deparaffinization process, deparaffinization solution (Qiagen GmbH) was used (incubation at 56°C for 3 min). Quantification of double-stranded DNA (dsDNA) and RNA was performed using a Qubit 4.0 Fluorometer (Thermo Fisher Scientific, Inc.) with a Qubit[™] dsDNA BR Assay kit (cat. no. Q32853; Thermo Fisher Scientific, Inc.) and a Qubit[™] RNA HS Assay kit (cat. no. Q32855; Thermo Fisher Scientific, Inc.), respectively. The quality of DNA was determined with an Illumina FFPE QC kit (cat. no. WG-321-1001; Illumina, Inc.). Only DNA samples with $\Delta\text{Cq} \leq 5$ and a concentration $\geq 10 \text{ ng}/\mu\text{l}$ were included. To assess the quality of extracted RNA, an Agilent 2100 Bioanalyzer with an Agilent RNA 6000 Nano Kit (cat. no. 5067-1511; Agilent Technologies, Inc.) was used. The main parameter indicating the quality of RNA samples was

the percentage of RNA fragments >200 nucleotides (DV_{200}). RNA samples with $DV_{200} > 30\%$ and a concentration $> 10 \text{ ng}/\mu\text{l}$ were accepted for library preparation.

Nucleic acid extraction and quality assessment of FF samples. Genomic DNA and total RNA were simultaneously extracted from FF tissues (volume of FF tissue $\sim 3.4 \text{ mm}^3$) using the AllPrep® DNA/RNA Micro kit (cat. no. 80284; Qiagen GmbH), according to the manufacturer's instructions. Quantification of dsDNA and RNA, was performed as aforementioned. The quality of DNA was determined using an Agilent 2100 Bioanalyzer with an Agilent DNA 12000 Kit (cat. no. 5067-1508; Agilent Technologies, Inc.). Samples with an average fragment size $\geq 4,500 \text{ bp}$ and a concentration $\geq 10 \text{ ng}/\mu\text{l}$ were analysed. To assess the quality of extracted RNA, an Agilent 2100 Bioanalyzer with an Agilent RNA 6000 Nano Kit (cat. no. 5067-1511; Agilent Technologies, Inc.) was used. RNA samples with $DV_{200} > 30\%$ and concentration $> 10 \text{ ng}/\mu\text{l}$ were accepted for library preparation.

Library preparation and sequencing of FFPE and FF samples. Library preparation was performed manually using the TSO 500 assay (Illumina, Inc.) according to the manufacturer's instructions. The TSO 500 assay is based on hybrid-capture chemistry and therefore requires a relatively large amount of input material with higher quality compared with amplicon-based chemistry. For library preparation, 70 ng DNA and 80 ng RNA were used. The first step in the process of DNA library preparation was DNA shearing using the Covaris® ML 230 instrument (Covaris, LLC) to obtain DNA fragments with an average length of $\sim 150 \text{ bp}$. RNA library preparation began with denaturation, annealing and two-step reverse transcription resulting in double-stranded cDNA. After these initial steps, DNA was sheared, and the corresponding cDNA was processed simultaneously based on the manufacturer's instructions. To assess the quantity and quality of libraries, the Qubit 4.0 Fluorometer was used with the Qubit™ dsDNA HS Assay kit (cat. no. Q32854; Thermo Fisher Scientific, Inc.) and the Agilent 2100 Bioanalyzer with the Agilent DNA 1000 Kit (cat. no. 5067-1505; Agilent Technologies, Inc.). Final libraries with a concentration $> 3 \text{ ng}/\mu\text{l}$ and a length of $\sim 260 \text{ bp}$ were normalised by bead-based normalisation to ensure a uniform library representation in the pooled libraries. The DNA pool consisted of eight DNA libraries and the cDNA pool contained eight corresponding cDNA libraries. After this process, the DNA and cDNA pools were mixed at a 4:1 ratio and diluted to the final loading concentration (1.5 pM). The paired-end sequencing runs were performed on the NextSeq 550 Dx (Illumina, Inc.) in research mode with a read length of $2 \times 101 \text{ bp}$.

Bioinformatic processing, tertiary analysis and post-processing. A custom script was used to prepare a sample sheet in the format required by PierianDx CGW (Pierian) based on the initial sequencing sample sheet. The sequencing run, utilizing the PierianDx-formatted sample sheet, was uploaded to an Amazon S3 bucket (public cloud storage; Amazon Web Services, Inc.) using CGW RunUploader (version 1.13; Pierian). This initiated the automatic conversion of bcl files to fastq files.

Subsequently, sample mapping and bulk accessioning files, required by PierianDx CGW, were generated using a custom script and uploaded to PierianDx CGW. Bioinformatic processing was conducted by PierianDx CGW using the LocalApp (version 2.2.0; Illumina, Inc.). Findings produced by the LocalApp were referred to as the raw findings. The tertiary analysis was performed using PierianDx CGW. Findings from the annotation by PierianDx CGW were referred to as the annotated findings.

Output files from PierianDx CGW processing, including QC reports for DNA and RNA (pdf files), tertiary analysis results (json files; report with results and case details) and variant call format files [vcf; main.vcf containing SNVs, CNVs, fusions and altered transcripts (AT)], were downloaded using API access to PierianDx CGW via custom scripts developed in R (version 4.0.5; Posit Software, PBC) (12).

The R library tabulizer (13) was used to create a script for extracting QC data from the QC pdf reports. Another R script was developed to extract information on SNVs, CNVs, fusions and AT from PierianDx CGW json reports, saving this data into csv files, using the R library jsonlite (14).

Statistical analysis. A flowchart illustrating the inclusion/exclusion of samples based on QC criteria was created using the R library DiagrammeR (15). The resulting html widget was saved with the R libraries DiagrammeRsvg (16) and rsvg (17). Small variants, CNVs, fusions and AT findings from the PierianDx CGW reports were analysed using a custom R script.

For exploratory data analysis, spaghetti plots were utilised to visualise the paired values of variant allele frequency (VAF) and depth for small variants. A Wilcoxon signed rank test was employed to test the null hypothesis that the median VAF value was the same in the FFPE subpopulation compared with the FF subpopulation, and the same test was applied to the depth. These tests were conducted for each diagnosis separately. Bar plots were used to display the counts of SNVs in FFPE and FF samples, categorised by type of cancer diagnosis, and the same approach was applied to CNVs, fusions and ATs. Venn diagrams were generated using the R library eulerr (18).

CNVs from the main.vcf files were visualised using bar plots showing the number of CNVs with fold change (FC) below the cut-off in both FFPE and FF samples, above the cut-off in FFPE and below the cut-off in FF tissues and above the cut-off in both FFPE and FF samples for each gene. The R library vcfR (19) was used to import main.vcf into R. The bias in FC estimates of FFPE relative to FF (or vice versa) was explored separately for the four subsets of patients: i1) For which FC was negative both in FFPE and FF; i2) positive in FFPE and negative in FF; i3) negative in FFPE and positive in FF; and i4) positive in both FFPE and FF) regardless of the gene. The FC in i1 (i2, i3 and i4) was explored using the box plot overlaid with swarm-plot, and the null hypothesis of the equality of medians in the FFPE/FF subpopulations was analysed using a paired Wilcoxon signed rank test. $P < 0.05$ was used to indicate a statistically significant difference.

Detailed data analysis reports generated using in-house R notebooks were uploaded to the following Mendeley repository: <https://data.mendeley.com/datasets/pw4h7zwvzz/1>.

Results

DNA and RNA quality metrics and assessment of NGS quality metrics. In total, DNA and RNA were extracted from a set of 100 FFPE samples and their corresponding FF samples. The median age of the samples was 17 months, ranging from 9-25 months. Samples with a portion of TCs >20% were included in the extraction process. The DNA extraction process from the FFPE tissues failed in 5/100 samples ($\Delta Cq > 5$), while DNA extraction from FF samples was successful for all samples. Among the RNA samples extracted from FFPE tissues, 20/100 did not meet the QC criteria ($DV_{200} < 30\%$). However, preliminary analysis of these samples showed that the storage period did not markedly impact the quality of the samples. The quality of RNA samples from paired FF tissues was lower compared with the high quality FF samples, but still met the required criteria. This suggested that the fixation process itself, particularly for tissues of lower quality, contributed to the degradation of RNA quality, hindering the analysis of FFPE samples. For the next step of library preparation, only samples that passed the initial QC for both DNA and RNA were used, resulting in 80 paired samples (Fig. 1).

The input for DNA and RNA library preparation was 70 ng genomic DNA and 80 ng RNA, respectively. The success of TSO 500 DNA and RNA library preparation was assessed based on QC criteria and thresholds from Appendix B of the Illumina Local Run Manager TruSight Oncology Comprehensive (EU) Analysis Module Workflow Guide (document no. 200008661; version 3; published July 2022) (20). DNA libraries were evaluated using values of contamination score, contamination P-value, median insert size, median exon coverage, PCT exon 50X, usable MSI sites, coverage median absolute deviation and median bin count CNV target (Fig. 2).

For a contaminated sample, both the contamination score value (3,106) and the contamination P-value (0.005) will be above their respective thresholds. Based on these values, 2 FFPE and 2 FF samples were identified as high-risk contaminated samples and were excluded from further analysis. The QC DNA metrics parameters low median exon coverage and higher coverage MAD were also monitored and resulted in the exclusion of 4 additional FF samples. In summary, based on QC DNA metrics, 8 samples were excluded (2 FFPE and 6 FF samples) from the analysed set. The evaluation of QC RNA metrics was then performed.

RNA libraries were evaluated using the values of the median coefficient of variation of the gene 500x, total target reads and median insert size. A total of 2 FF samples did not meet the required number of total on-target reads and 1 FFPE sample did not exceed the required value for median insert size (Fig. 3).

To facilitate a comprehensive comparison of all monitored parameters and findings across DNA and RNA analyses, only samples that met all QC values for both DNA and RNA in both FFPE and FF samples were included for the final comparisons. Through this selection process, 11 patients were excluded from the initial set of 80 patients. Therefore, 69 paired samples (23 BC, 22 CRC and 24 LC samples) that passed the filters were included in the analysis. These 138 samples (69 pairs) were analysed for small variants, MSI, TMB, fusions, splice variants

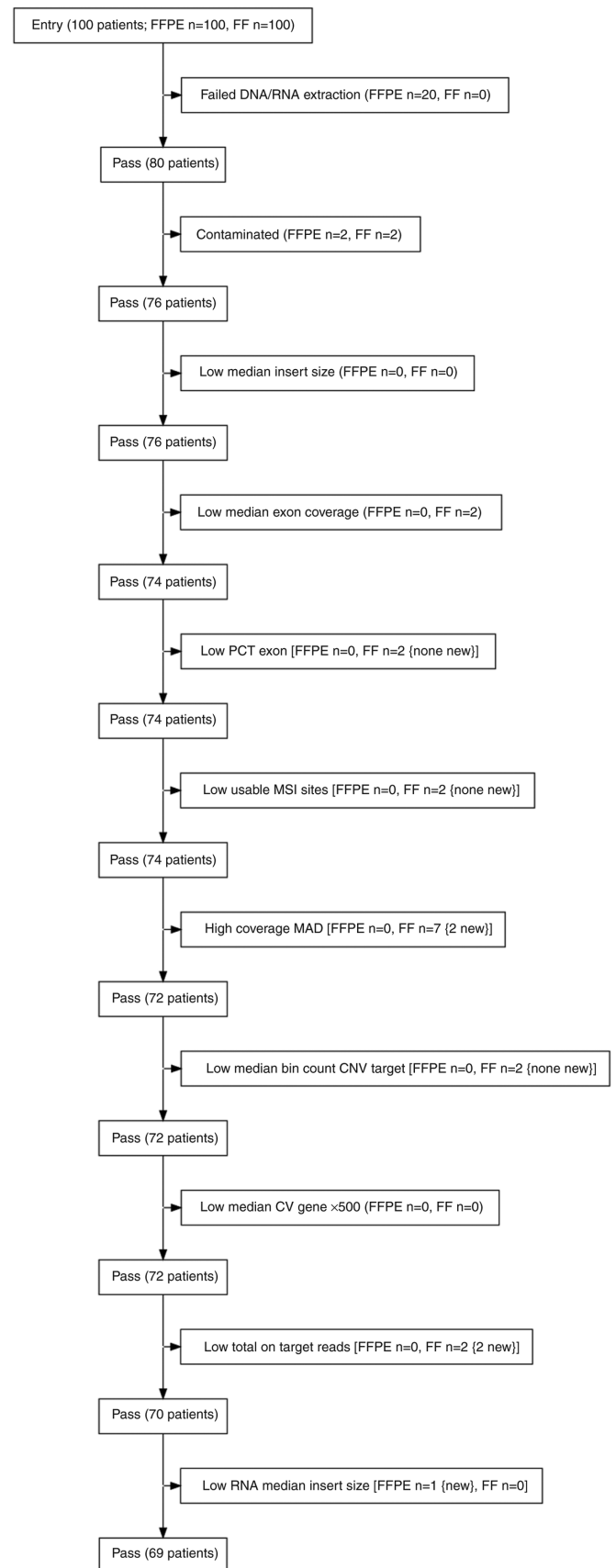


Figure 1. Flowchart of the inclusion and exclusion process of samples based on quality control criteria and thresholds from Appendix B of the Illumina Local Run Manager TruSight Oncology Comprehensive (EU) Analysis Module Workflow Guide (document no. 200008661; version 3; published July 2022). FFPE, formalin-fixed paraffin embedded; FF, fresh frozen; PCT, percent; MSI, microsatellite instability; MAD, median absolute deviation; CNV, copy number variation; CV, coefficient of variation.

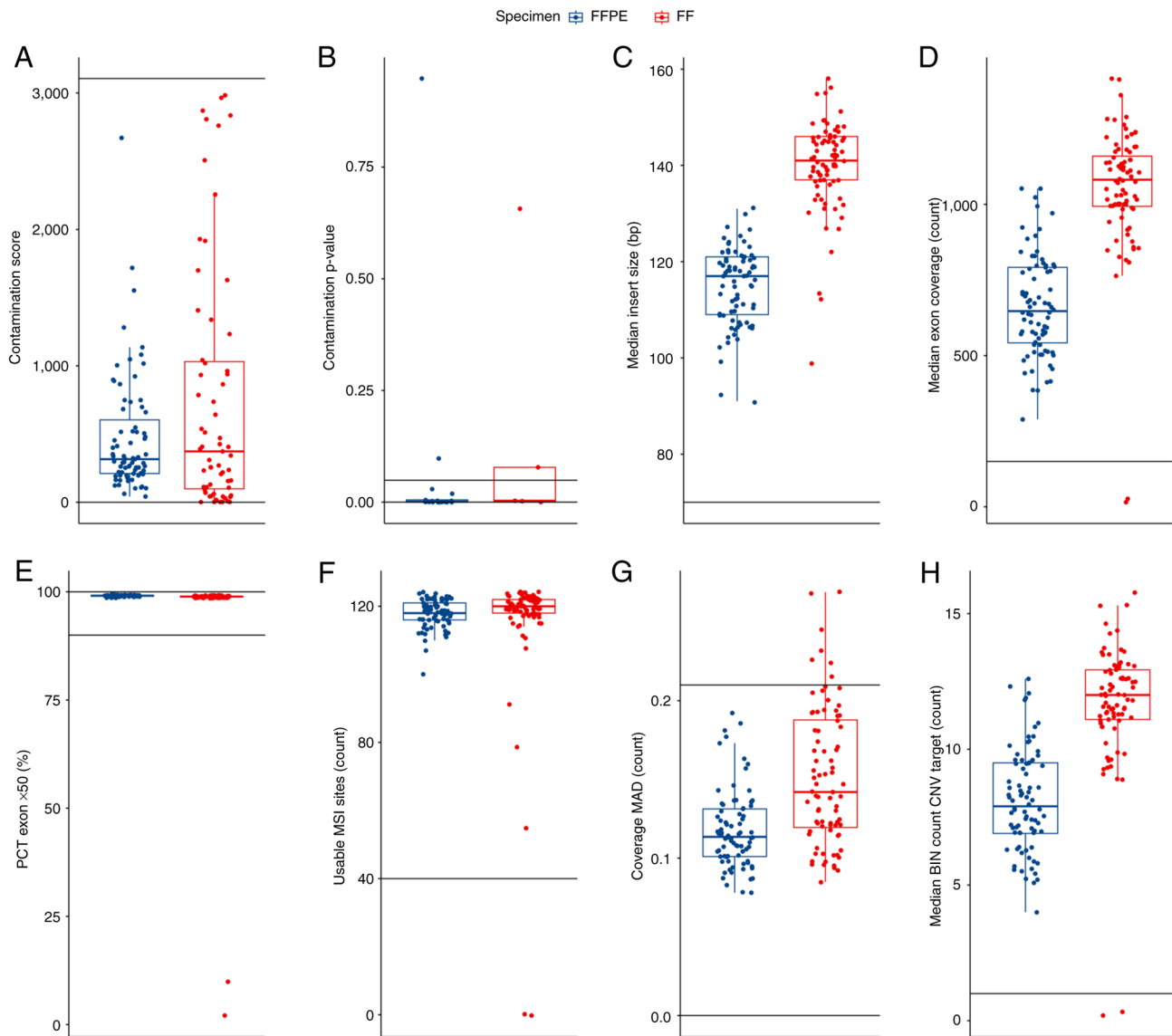


Figure 2. Quality control DNA metrics for the 80 patient samples from the present study that were sequenced. The data are visualized by boxplot overlaid with swarmplot. In each panel, the cut-offs delineating the range of acceptable values are plotted as horizontal lines and the values of the metrics for FFPE (blue) and FF (red) tissues are presented. (A) Contamination score of the subset of samples with a value <3106. (B) Contamination P-values for the samples with a contamination score >3106. (C) Median insert size. (D) Median exon coverage. (E) PCT exon 50X. (F) Usable MSI sites. (G) Coverage MAD. (H) Median BIN count CNV target. The boxplot displays several key statistical measures: The horizontal line within the box indicates the median (Q2) of the dataset. The lower and upper edges of the box represent Q1 and Q3, respectively, encompassing the IQR which contains the central 50% of the data. The whiskers extend from the box to show variability outside this range, typically reaching up to 1.5 times the IQR from Q1 and Q3, while any points beyond this range are plotted as outliers. FFPE, formalin-fixed paraffin-embedded; FF, fresh frozen; MAD, median absolute deviation; MSI, microsatellite instability; PCT, percent; CNV, copy number variation; BIN, interval or region of the genome into which sequencing data is grouped for analysis; IQR, interquartile range; Q1, first quartile; Q3, third quartile.

and CNVs using the TSO 500 panel, with data processed through the Illumina TruSight Oncology Local App pipeline (version 2.2) and PierianDx CGW. The median values of QC DNA and RNA metrics, values of recommended thresholds and P-values from the two-sample paired Wilcoxon test for samples that passed QC were analysed (Table I). Significantly increased values for most observed parameters in FF samples were observed, except for DNA usable MSI sites, RNA total on-target reads and RNA median insert size. Notably, the DNA median insert size, DNA median exon coverage and RNA median CV gene 500x indicated higher quality for both DNA and RNA extracted from FF tissue compared with FFPE samples.

Small variants. The TSO 500 pipeline enables the detection of small variants, including SNVs, multi-nucleotide variants (MNVs) up to 3 bp in length and insertions and deletions up to 25 bp in length, in most of the coding regions of 523 selected genes (20). In the present comparative study, Tier IA and IB findings were focussed on, as reported by PierianDx CGW, as these hold the highest diagnostic significance.

In 25 paired samples (36%; 3 BC, 10 LC and 2 CC pairs) no small variants were detected in Tiers IA or IB. In the remaining 44 pairs, a total of 133 Tier IA/IB variants were identified (Fig. 4). A complete list of detected small variants can be found in the supplementary file (<https://data.mendeley.com/datasets/pw4h7zwvzz/1>). A total of 130 variants were

Table I. Median quality control values from Appendix B of the Illumina Local Run Manager TruSight Oncology Comprehensive (EU) Analysis Module Workflow Guide (document no. 200008661; version 3; published July 2022).

Characteristic	FFPE, median	FF, median	Recommended threshold	P-value
DNA contamination score	299	538	0.000-3,106.000	0.003
DNA contamination P-value	1	1	0.000-0.049	<0.001
DNA median insert size	118	140	≥70.000	<0.001
DNA median exon coverage	651	1,075	≥150.000	<0.001
DNA percentage exon 50x, %	99.1	98.9	90.000-100.000	<0.001
DNA usable microsatellite instability sites	118	120	≥40.000	0.049
DNA coverage median absolute deviation	0.11	0.14	0.000-0.210	<0.001
DNA median bin count copy number variant target	7.8	11.8	≥1.000	<0.001
RNA median coefficient of variation gene 500x	59.2	64.2	0.000-93.000	<0.001
RNA total on-target reads	17,895,298	18,146,831	>9,000,000.000	0.500
RNA median insert size	114	115	>80.000	0.030

P-values were calculated using the two-sample paired Wilcoxon test on 69 pairs of samples that passed quality control.

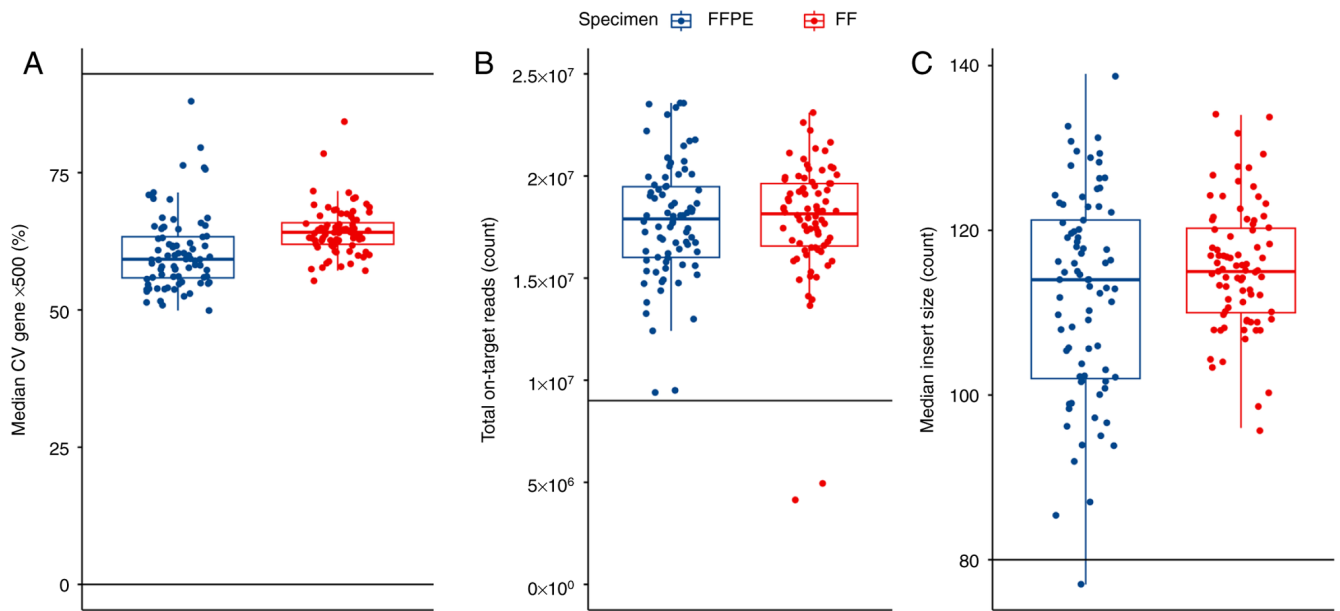


Figure 3. Quality control RNA metrics for the 80 patient samples from the present study that were sequenced. The data are visualized by boxplot overlaid with swarmplot. In each panel, the cut-offs delineating the range of acceptable values are plotted as horizontal lines and the values of the metrics for FFPE (blue) and FF (red) tissues are presented. (A) Median coefficient of variation of gene 500x, (B) Total on-target reads. (C) Median insert size. The boxplot displays several key statistical measures: The horizontal line within the box indicates the median (Q2) of the dataset. The lower and upper edges of the box represent Q1 and Q3, respectively, encompassing the IQR which contains the central 50% of the data. The whiskers extend from the box to show variability outside this range, typically reaching up to 1.5 times the IQR from Q1 and Q3, while any points beyond this range are plotted as outliers. FFPE, formalin-fixed paraffin-embedded; FF, fresh frozen; IQR, interquartile range; Q1, first quartile; Q3, third quartile; Q2, median.

detected in FFPE and paired FF samples. The discordant cases consisted of 2 FFPE+, FF- and 1 FFPE-, FF+ variants, where + indicates the presence of the variant, and - indicates the absence of the variant (Fig. 5). In general, longer insert sizes make it easier for software algorithms to align reads. Therefore, longer DNA and RNA insert sizes are often correlated with better performance, mainly due to higher coverage. In the present sample set, significantly longer DNA insert sizes for FF samples were observed compared with FFPE samples,

with an average of 118 bp for FFPE and 140 bp for FF samples. This indicated higher quality inputs from FF samples, as sample quality is a key determinant of final insert sizes. When high- and low-quality inputs are processed in parallel, they yield libraries with higher and lower performance, respectively. However, it was demonstrated that the TSO 500 assay effectively identified small variants with a high concordance of 97.7% (130/133) for both FFPE and FF samples, regardless of the difference in the DNA median insert size.

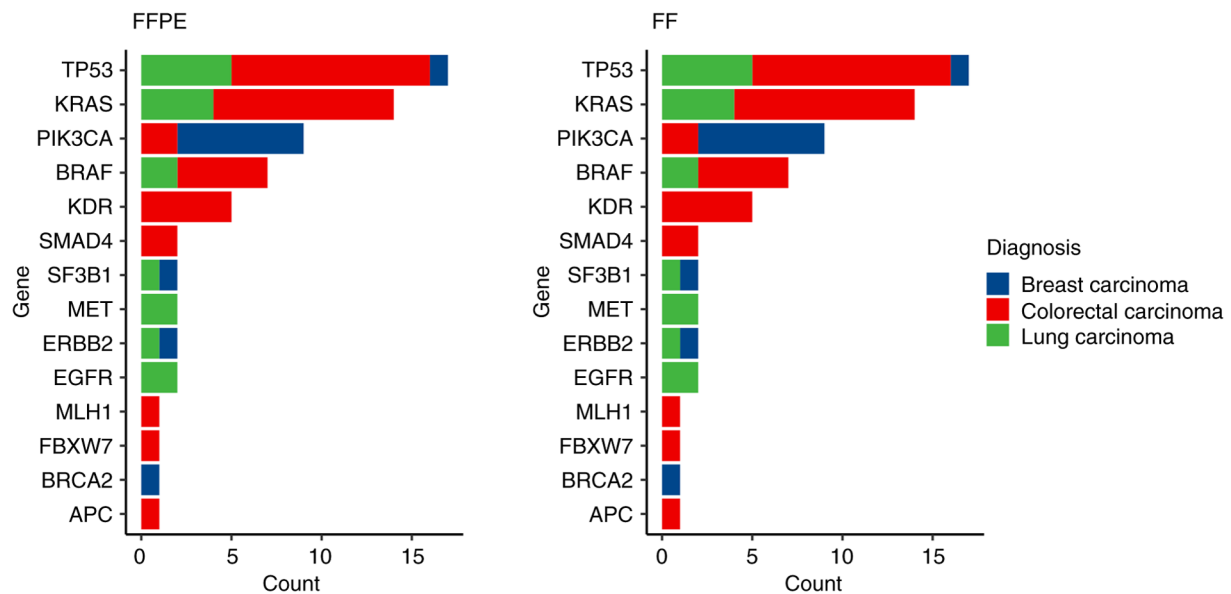


Figure 4. Bar plots of genes in which mutations from tiers IA and IB were detected, with the number of small variants from tiers IA and IB identified in FFPE and FF tissues categorised by type of diagnosis. FFPE, formalin-fixed paraffin-embedded; FF, fresh frozen.

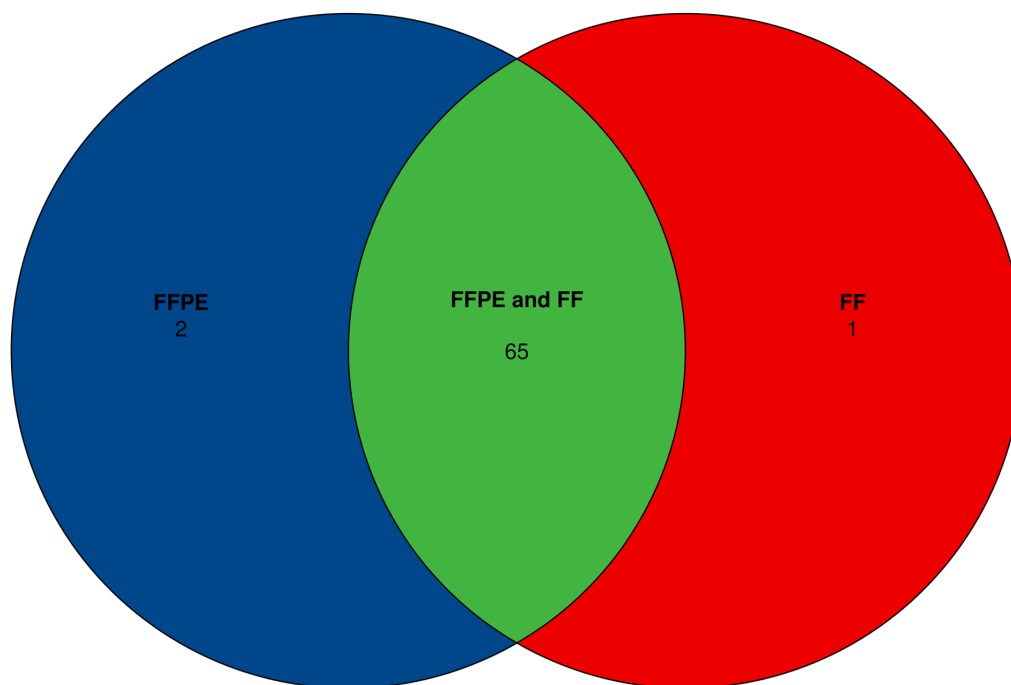


Figure 5. Venn diagram of small variants (tiers IA and IB) in FFPE only (blue), FF only (red) and both FFPE and FF (green) tissues. The total number of small variants in tiers IA and IB is 133. FFPE, formalin-fixed paraffin-embedded; FF, fresh frozen.

For a comprehensive evaluation of the performance of the TSO 500 assay, VAF and depth values were analysed, which are crucial for identifying small variants (Table II). These results demonstrated significantly increased values for both VAF and depth parameters in FF samples across all analysed cancer types compared with FFPE samples.

Microsatellite instability. To determine MSI status (MSI-stable vs. MSI-high), 130 homopolymer sites in the non-coding regions are monitored in the TSO 500 panel. The final MSI score is calculated as the number of unstable sites divided by

the total number of usable sites, which are sites with sufficient coverage. A sample is considered MSI-high if its MSI score is $\geq 20.00\%$ (20). MSI scores were compared for 63 pairs of samples, because the software was unable to determine the MSI status for some samples and these pairs were subsequently excluded. FFPE-, FF- accounted for 58 pairs, 0 pairs were FFPE+, FF-, 1 pair was FFPE-, FF+ and 4 pairs were FFPE+, FF+, where '+' indicated MSI-high status and '-' indicated MSI-stable status (Fig. 6). All FFPE+, FF+ samples were CRC, which was consistent with the occurrence of MSI-high cases in a previously published report (21). The FFPE-, FF+ discordant

Table II. Descriptive statistics and P-values of VAF and sequencing depth for small variants in tiers IA and IB, which are present in both FFPE and FF samples.

A, Breast carcinoma			
Characteristic	FFPE	FF	P-value
Number of variants , n	11	11	-
VAF, median % (IQR)	20 (18, 29)	39 (33, 53)	<0.001
Depth, median x (IQR)	810 (602, 1,025)	1,054 (819, 1,144)	0.042
B, Colorectal carcinoma			
Characteristic	FFPE	FF	P-value
Number of variants , n	38	38	-
VAF, median % (IQR)	27 (21, 35)	40 (22, 60)	0.009
Depth, median x (IQR)	524 (432, 630)	948 (787, 1,087)	<0.001
C, Lung carcinoma			
Characteristic	FFPE	FF	P-value
Number of variants , n	14	14	-
VAF, median % (IQR)	22 (19, 34)	49 (28, 52)	0.002
Depth, median x (IQR)	616 (508, 910)	1,188 (872, 1,404)	<0.001
D, Overall			
Characteristic	FFPE	FF	P-value
Number of variants , n	63	63	-
VAF, median % (IQR)	26 (19, 34)	41 (25, 58)	<0.001
Depth, median x (IQR)	568 (452, 708)	994 (807, 1,188)	<0.001
VAF, variant allele frequency; FFPE, formalin-fixed paraffin-embedded; FF, fresh frozen.			

pair was from LC samples with 19.2% MSI unstable sites, which was just below the 20% MSI cut-off point. The concordance of MSI status between FFPE and FF samples was 98.4%.

Tumour mutational burden. The TMB score was generated from the gVCF files based on small variant calling, which included analysis of SNVs, insertions and deletions with VAF >5%. A crucial step in this process is the removal of variants with >50 COSMIC annotations from the analysis. These hotspot mutations, which are under positive selection during cancer progression, have the potential to skew the TMB score generated by the TSO 500 pipeline (20). In summary, TMB values were returned by LocalApp for 66 paired samples with the following results: 51 FFPE-, FF-, 3 FFPE-, FF+, 2 FFPE+, FF- and 10 FFPE+, FF+ pairs, where '+' indicated TMB high status, and '-' indicated TMB low status (Fig. 7). Almost all the discordant samples had TMB values near the cut-off (range, 8.6-9.4), except 1 LC sample which was FFPE-, FF+ with a TMB value of 4.7, which indicated a high degree of concordance between the FFPE and FF samples (92.4%).

Fusions. For fusion calling, unique reads were used, with ≥ 5 unique supporting reads required to filter for high-confidence variants. 'Min supporting reads' was defined as five for samples with <26 million reads, with an additional read required for every 10 million reads >16 million. This was performed to prevent false positives in very high-depth samples (20). In the present sample set, the following types of fusions were identified from Tiers IA and IB: *ESR1-CCND1*, *ESR1-HFMI*, *KIF5B-RET* and *EML4-ALK*. Of these, 1 pair of samples was FFPE+, FF-, 2 pairs were FFPE+, FF+ and 1 pair was FFPE-, FF+, (concordance 50%), where '+' indicated the presence of the fusion, and '-' indicated the absence of the fusion. Due to the low number of detected fusions, the present analysis subsequently focused on identified fusions highlighted by PierianDx CGW (including Tiers IIC and IID). This approach allowed us to determine the concordance more accurately. A total of three additional types of fusion that belonged to Tier IIC or IID (*EWSR1-BEND2*, *RPS6KB1-VMPI* and *GPR107-JAK2*), with 1 pair of samples recorded as FFPE-, FF+ and 2 pairs as FFPE+, FF+, which confirmed the trend of analysis of fusion from Tiers IA and IB.

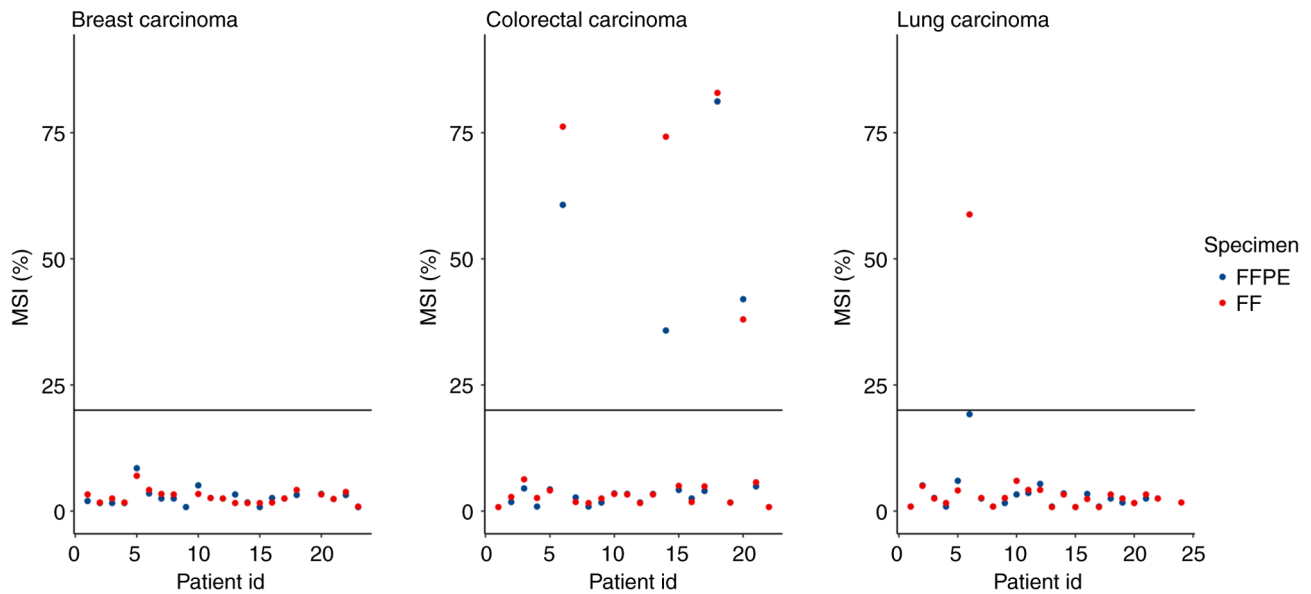


Figure 6. MSI index plot by diagnosis with the cut-off set to 20%. The values of the MSI score for FFPE (blue) and FF (red) tissues are presented. FFPE, formalin-fixed paraffin-embedded; FF, fresh frozen; MSI, microsatellite instability.

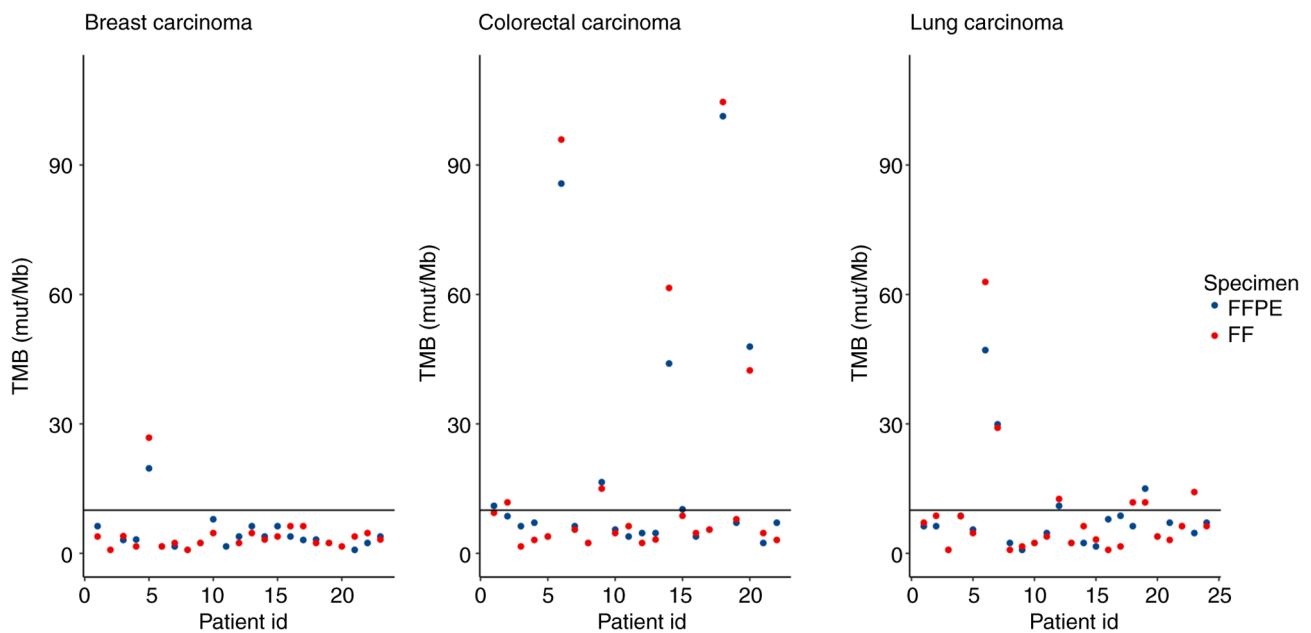


Figure 7. TMB index plot by diagnosis with the cut-off set 10%. The values of TMB for FFPE (blue) and FF (red) are presented. FFPE, formalin-fixed paraffin-embedded; FF, fresh frozen; TMB, tumour mutational burden; mut/Mb, number of mutations per megabase.

Splice variants. The analysis of splice variants using TSO 500 focused on the following three variant types: MET Exon 14 skipping, EGFRvIII and ARv7. A splice variant is detected if it is supported by at ≥ 24 reads (20). A total of two types of splice variants were found in Tiers IA and IB: In gene AR ($n=4$, all in BC samples) and one in MET in an LC sample. All findings belonged to discordant samples: 2 samples were FFPE+, FF- and 3 samples were FFPE-, FF+, where '+' indicated the presence of the splice variant and '-' indicated the absence of the splice variant. These results suggested a lack of concordance in the detection of clinically relevant splice variants in the present sample set.

Copy number variations. A total of 59 genes were analysed for CNV calling in the TSO 500 panel. The amplification and deletion limit of detection was a 2.2- and 0.5-fold increase and decrease, respectively. Each gene exhibits a unique noise profile, necessitating specific thresholds for calling amplifications and deletions (20). In the first phase of CNV analysis, CNVs from Tiers IA and IB were analysed. Out of the total number of detected clinically relevant CNVs ($n=74$), all were amplifications (Fig. 8). A total of 11 CNVs were in FFPE+, FF- discordant samples, and 17 CNVs were in FFPE-, FF+ discordant samples (Fig. 9A). This represented 62.2% concordance in the identification of the aforementioned types of CNVs. Due to the fixed

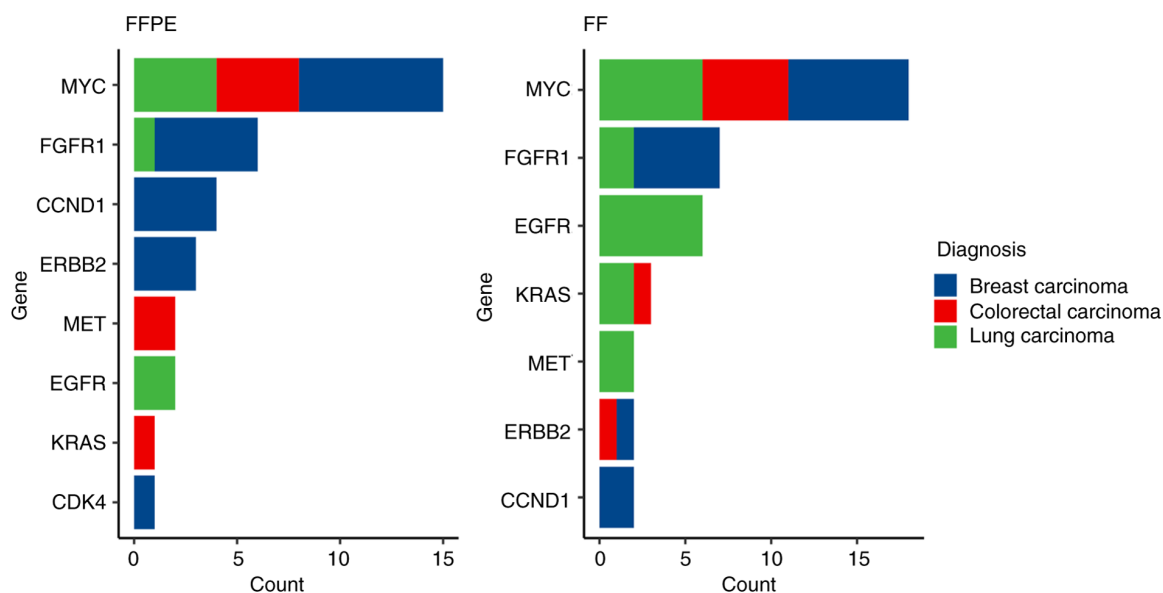


Figure 8. Bar plot of copy number variations (tiers IA and IB) in FFPE and FF tissues categorised by type diagnosis. FFPE, formalin-fixed paraffin-embedded; FF, fresh frozen.

frame of analysis for CNVs per sample, all CNVs were analysed across the 59 genes (Fig. 9B). A total of 337 amplifications were detected, which included discordant CNVs and FFPE+, FF- (n=24) and FFPE-, FF+ (n=143) samples. The remaining amplifications (n=170) were found in both paired FFPE and FF samples (overall concordance 50.4%). The counts of the four combinations of agreement/disagreement between FC of CNVs in FFPE vs. FF for all 69 paired samples were measured (Fig. 10). A different cut-off of the FC was applied for each gene, following the recommendations of the kit manufacturer. The four combinations analysed together were FFPE-, FF+, FFPE+, FF+, FFPE+, FF- and FFPE-, FF-, where '+' indicated that the FC was above the cut-off, and '-' indicated that it was below the cut-off value.

Concordance of raw CNV findings in paired FFPE and FF samples. To investigate the bias in FC values between FFPE and FF (or vice versa) from raw findings obtained by LocalApp, four patient subsets were considered. The subsets (i1-i4) were identified for each gene, and all patients and genes in each subset were then analysed together. The data were visualised using boxplot overlaid with swarmplot (Fig. 11). The median FC in FFPE, median FC in FF, median of paired differences (FFPE vs. FF) and the P-value from Wilcoxon's paired test for the four subsets were analysed (Table III). The observed median of the paired differences (FFPE vs. FF) of FC for subsets i1, i2, i3 and i4 were -0.022, 0.386, -0.389 and -0.245, respectively. In all four cases, $P < 0.0001$. Subsets i2 and i3 showed a nearly identical levels of differences between the FC in FFPE and FF, which was 0.368 and -0.389, respectively. In subsets i1, i3 and i4, the median of the paired differences (FFPE vs. FF) of FC values was negative, indicating a systematic occurrence of higher FC values in FF samples.

Discussion

The present study focused on a comprehensive comparison of NGS quality metrics and concordance in the detection of

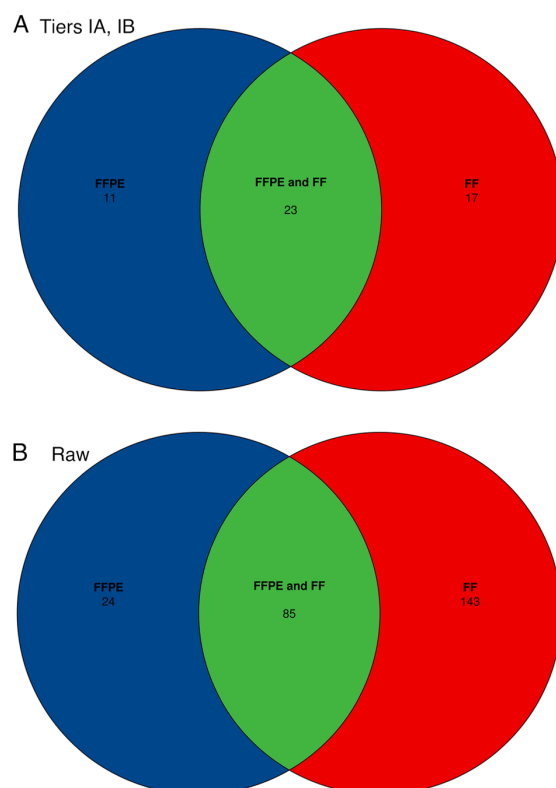
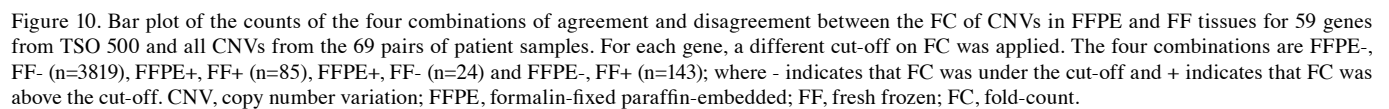


Figure 9. Venn diagrams of CNVs. (A) Venn diagram of CNVs (tiers IA and IB); in FFPE (blue), FF (red) and both FFPE and FF (green) tissues. The total number of CNVs in tiers IA and IB is 74. (B) Venn diagram of all detected amplifications in FFPE (blue), FF (red) and both FFPE and FF (green) tissues. The total number of detected amplifications is 337. FFPE, formalin-fixed paraffin-embedded; FF, fresh frozen; CNVs, copy number variations.

clinically relevant variants (small variants, indels, splice variants, TMB, MSI and CNVs) using TSO 500 in paired FFPE and FF samples. The TSO 500 assay was designed to analyse nucleic



The TSO 500 is a hybrid capture NGS panel that requires a higher quantity and quality of NAs compared with smaller amplicon-based panels. Based on our pilot testing phase and the manufacturer's recommendations, only analysed DNA samples with a $\Delta C_q \leq 5$ and an input quantity of 70 ng were analysed. RNA samples were required to meet $DV_{200} \geq 30\%$ and an input quantity of 80 ng. A total of 20/100 archived FFPE

For the detection of small variants, MSI, TMB, fusions, splice variants and CNVs using the TSO500 panel, the Illumina TruSight Oncology Local App pipeline (version 2.2) was utilised. The results were subsequently annotated using the PierianDx CGW, which classified small variants, fusions, splice variants and CNVs into tiers. No small variants from Tier IA or IB were detected in 25 pairs of samples (36%) (6 BC, 3 LC and 2 CC samples).

Table III. Paired comparisons of FC in all four combinations of CNV findings.

Type of CNV finding	Median FC in FFPE	Median FC in FF	Median paired difference (FFPE-FF)	P-value
FFPE-, FF-	0.989	1.016	-0.022	<0.0001
FFPE+, FF-	1.57	1.232	0.386	<0.0001
FFPE-, FF+	1.203	1.564	-0.389	<0.0001
FFPE+, FF+	1.692	1.876	-0.245	<0.0001

FC, fold change; FFPE, formalin-fixed paraffin-embedded; FF, fresh frozen; CNV, copy number variation.

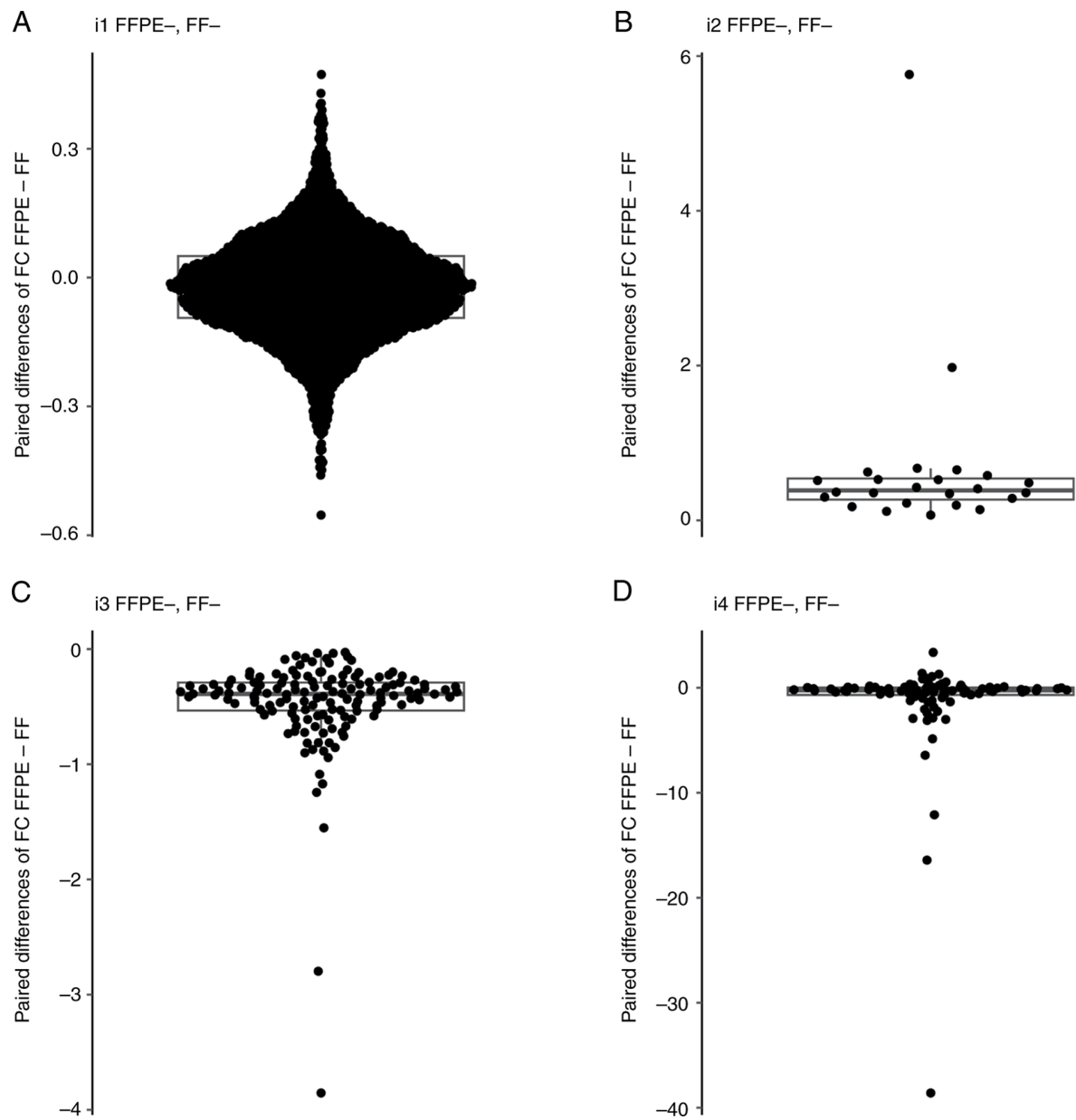


Figure 11. Boxplots of FC values. (A) Boxplot overlaid with swarm plot of paired difference of FC values (FFPE-FF) for the patients and genes in subset i1. (B) Boxplot overlaid with swarm plot of paired difference of FC values (FFPE-FF) for the patients and genes in subset i2. (C) Boxplot overlaid with swarm plot of paired difference of FC values (FFPE-FF) for the patients and genes in subset i3. (D) Boxplot overlaid with swarm plot of paired difference of FC values (FFPE-FF) for the patients and genes in subset i4. The boxplot displays several key statistical measures: The horizontal line within the box indicates the median (Q2) of the dataset. The lower and upper edges of the box represent Q1 and Q3, respectively, encompassing the IQR, which contains the central 50% of the data. The whiskers extend from the box to show variability outside this range, typically reaching up to 1.5 times the IQR from Q1 and Q3, while any points beyond this range are plotted as outliers. FFPE, formalin-fixed paraffin-embedded; FF, fresh frozen; FC, fold change; IQR, interquartile range; Q1, first quartile; Q3, third quartile; Q2, median.

which aligned with previous analyses by Ottestad *et al* (4) who reported that 37% of samples exhibited no detectable mutations in the analysed genes. In the remaining 44 samples, 133 small variants were identified, with 130 occurring in pairs and 3 classified as discordant findings. The results demonstrated a high concordance value of 97.7%. For a more comprehensive analysis of small variant results, VAF and depth values were examined with respect to the type of tissue used. The depth value was significantly higher in FF samples compared with FFPE samples, 568 vs. 994x, respectively, which was related to the higher quality of the input material. The quality of the material also correlated closely with the VAF value, which reached almost double in FF samples, 26 vs. 41%. This is because algorithms investigating the input data can more efficiently align reads, thereby obtaining a larger set of sequences supporting variant presence and achieving higher test sensitivity. The detection capability of TSO 500 of small variants was not affected in the case of analysing samples with a portion of TCs >20%. However, if lower-quality samples with a low proportion of neoplastic cells are used, the advantage of FF samples may be more apparent. Additional important genomic biomarkers used to identify patients who may benefit from immune checkpoint inhibitor treatment are MSI and TMB. High concordance rates were observed for MSI and TMB, with values of 98.4 and 92.4%, respectively. Additionally, most of the discordant samples identified in the TMB analysis were very close to the cut-off value.

A different outcome was observed with the detection of fusions and splice variants. PierianDx CGW reported a total of four fusions and five splice variants in Tiers IA and IB. Half of the samples were evaluated as discordant for fusions, and no concordance was observed for splice variants. This could potentially be attributed to the small number of identified variants. However, even when all findings were analysed, including the variants from raw findings returned by LocalApp, the results did not differ substantially.

Within the present sample cohort, no whole-gene deletions were detected. All the identified CNVs were amplifications; however, lower concordance rates were observed. Specifically, a 62.2% concordance for clinically relevant CNVs was observed from Tiers IA and IB and 50.4% concordance for all identified CNVs. Giacobbe *et al* (1) reported an issue with CNV detection when using TSO 500. One of the suggested reasons for the insufficient detection was that the Illumina LocalApp algorithm is designed for whole-gene analysis and not for exon-level resolution, which is particularly important for the BRCA1/2 genes. In the case of BRCA1/2, CNVs also occur at the exon level, not on the whole gene, which makes it more difficult or even impossible to detect them using the TSO 500 assay. The study also encountered coverage-related issues that could impact the detection of small variants and CNV identification. Similar to previous studies focusing on whole-exome sequencing (26,27), Giacobbe *et al* observed that low and nonuniform coverage can compromise the ability to detect this type of genetic variation. The samples analysed in the present study met the quality criteria that would indicate coverage-related issues. These parameters included High Coverage_MAD values (>0.21), which could be due to poor input DNA quality, poor enrichment during library preparation or the use of non-FFPE samples and Low Median_BIN_COUNT_CNV_Target values (<1.0), suggesting low coverage in target regions, possibly due

to poor sample quality, poor library preparation or insufficient sequencing output (20). Although CNV calling in the Illumina Local App using CRAFT (28) is specifically validated for FFPE samples, effective CNV identification should be achievable for all samples that meet the aforementioned QC metrics.

To investigate the bias in paired FC values between FFPE and FF (or vice versa) from raw findings obtained by LocalApp, 4 patient subsets were considered. The subsets i1 (FFPE-, FF-), i2 (FFPE+, FF-), i3 (FFPE-, FF+) and i4 (FFPE+, FF+) were identified for each gene, and all patients and genes in each subset were analysed together. In the case of discordant findings (i.e., subsets i2 and i3), almost identical medians of paired differences in FC values between FFPE and FF samples were observed: 0.368 and -0.389, respectively. In subsets i1, i3 and i4, the medians of paired differences (FFPE minus FF) in FC values were negative, indicating a systematic occurrence of higher FC values in FF samples. Therefore, except for cases of CNVs in the FFPE+, FF- subset, the FC values were systematically higher in FF samples compared with those in FFPE samples. The present study was unable to determine whether the systematic bias was due to the algorithm for CNV calling used in the LocalApp or if it reflected a genuine difference related to the higher quality of input genetic material. Repeated analysis of inconsistent results confirmed the previous findings. To address this, it is therefore necessary to conduct intra- and inter-laboratory validation of TSO 500 CNV detection in FF samples on an alternative testing platform to rule out technical issues. For example, methods such as array comparative genomic hybridization, digital droplet PCR, or whole-genome sequencing could be employed.

To the best of our knowledge, the present study is the first to report the use of the TSO 500 assay in paired FFPE and FF tumour tissue samples. Comparisons of NGS quality metrics and the concordance in the detection of clinically relevant variants were annotated using the Pierian Dx CGW. Based on these results, it could be suggested that it is more advantageous to use FF tissues to detect small variants and TMB and MSI biomarkers using the TSO 500 assay, thus reducing the number of no-calls due to low-quality NAs. For cancer types where accurate detection of CNVs is critical, intra- and inter-laboratory validation should be considered.

Acknowledgements

Not applicable.

Funding

This publication was created under the Operational Programme Integrated Infrastructure for the project: Integrative strategy in development of personalized medicine of selected malignant tumours and its impact on quality of life (project code ITMS 2014+, 313011V446), co-financed by the European Regional Development Fund.

Availability of data and materials

The raw sequencing data can be found in the Sequence Read Archive under accession number PRJNA1197108 or at the following URL: <https://www.ncbi.nlm.nih.gov/sra/PRJNA1197108>.

Authors' contributions

ZD, MG, EH, DL and LP had substantial contributions to the conception and design of the work. KT, KL, ZD, KB, EK, TR, AD, JM, PM and MS processed the samples. DL and AH completed the molecular analysis. MG, DL and AH analysed the data. DL, MG, AH, LP and EH prepared the manuscript. DL and EH confirm the authenticity of all the raw data. All authors read and approved the final version of the manuscript.

Ethics approval and consent to participate

Ethics approval for the study was obtained from the Ethics Committee of the Jessenius Faculty of Medicine in Martin (no. EK 79/2020; Martin, Slovakia). The study was performed in accordance with the ethical standards as written in the 1964 Declaration of Helsinki and its later amendments.

Patient consent for publication

Not applicable.

Competing interests

The authors declare that they have no competing interests.

References

- Giacò L, Palluzzi F, Guido D, Nero C, Giacomini F, Duranti S, Bria E, Tortora G, Cenci T, Martini M, *et al.*: A computational framework for comprehensive genomic profiling in solid cancers: The analytical performance of a high-throughput assay for small and copy number variants. *Cancers (Basel)* 14: 6152, 2022.
- Froyen G, Geerdens E, Berden S, Cruys B and Maes B: Diagnostic validation of a comprehensive targeted panel for broad mutational and biomarker analysis in solid tumors. *Cancers (Basel)* 14: 2457, 2022.
- Conroy JM, Pabla S, Glenn ST, Seager RJ, Van Roey E, Gao S, Burgher B, Andreas J, Giamo V, Mallon M, *et al.*: A scalable high-throughput targeted next-generation sequencing assay for comprehensive genomic profiling of solid tumors. *PLoS One* 16: e0260089, 2021.
- Ottstad AL, Huang M, Emdal EF, Mjelle R, Skarpeteig V and Dai HY: Assessment of two commercial comprehensive gene panels for personalized cancer treatment. *J Pers Med* 13: 42, 2022.
- Pestinger V, Smith M, Sillo T, Findlay JM, Laes JF, Martin G, Middleton G, Taniere P and Beggs AD: Use of an integrated pan-cancer oncology enrichment next-generation sequencing assay to measure tumour mutational burden and detect clinically actionable variants. *Mol Diagn Ther* 24: 505, 2020.
- Meireles SI, Cruz MV, de Godoy CD and de Testagrossa L: Performance of non-formalin fixed paraffin embedded samples in hybrid capture and amplicon next-generation sequencing panels. *Diagn Cytopathol* 52: 171-182, 2024.
- Betje J, Kerr G, Miersch T, Leible S, Erdmann G, Galata CL, Zhan T, Gaiser T, Post S, Ebert MP, *et al.*: Amplicon sequencing of colorectal cancer: Variant calling in frozen and formalin-fixed samples. *PLoS One* 10: e0127146, 2015.
- Robbe P, Popitsch N, Knight SJL, Antoniou P, Becq J, He M, Kanapin A, Samsonova A, Vavoulis DV, Ross MT, *et al.*: Clinical whole-genome sequencing from routine formalin-fixed, paraffin-embedded specimens: Pilot study for the 100,000 Genomes Project. *Genet Med* 20: 1196-1205, 2018.
- De Paoli-Iseppi R, Johansson PA, Menzies AM, Dias KR, Pupo GM, Kakavand H, Wilmott JS, Mann GJ, Hayward NK, Dinger ME, *et al.*: Comparison of whole-exome sequencing of matched fresh and formalin fixed paraffin embedded melanoma tumours: implications for clinical decision making. *Pathology* 48: 261-266, 2016.
- Kerick M, Isau M, Timmermann B, Sultmann H, Herwig R, Krobisch S, Schaefer G, Verdorfer I, Bartsch G, Klocker H, *et al.*: Targeted high throughput sequencing in clinical cancer settings: Formaldehyde fixed-paraffin embedded (FFPE) tumor tissues, input amount and tumor heterogeneity. *BMC Med Genomics* 4: 68, 2011.
- Fielding DI, Dalley AJ, Singh M, Nandakumar L, Lakis V, Chittoory H, Fairbairn D, Patch AM, Kazakoff SH, Ferguson K, *et al.*: Evaluating diff-quick cytology smears for large-panel mutation testing in lung cancer-predicting DNA content and success with low-malignant-cellularity samples. *Cancer Cytopathol* 131: 373-382, 2023.
- R Core Team (2021) R: A language and environment for statistical computing. R Foundation for Statistical Computing, Vienna, 2021.
- tabulizer: Bindings for Tabula PDF Table Extractor Library. R package version 0.2.2.
- Ooms J: The jsonlite Package: A practical and consistent mapping between JSON data and R Objects 2014.
- Iannone R and Roy O: DiagrammeR: Graph/Network Visualization. 2024.
- Iannone R: DiagrammeRsvg: Export DiagrammeR Graphviz Graphs as SVG. 2016.
- Ooms J and Brüggemann S: Render SVG images into PDF, PNG, (Encapsulated) PostScript, or Bitmap Arrays 2023.
- Larsson J, Godfrey AJR, Gustafsson P, Eberly DH, Huber E and Privé F: Area-proportional euler and venn diagrams with ellipses. 2024.
- Knaus BJ and Grünwald NJ: vcfr: A package to manipulate and visualize VCF format data in R. *Mol Ecol Resour* 17: 44-53, 2017.
- Local run manager trusight oncology comprehensive (EU) analysis module. 2022.
- Bonneville R, Krook MA, Kautto EA, Miya J, Wing MR, Chen HZ, Reeser JW, Yu L and Roychowdhury S: Landscape of microsatellite instability across 39 cancer types. *JCO Precis Oncol* 17: 00073, 2017.
- Baum JE, Zhang P, Hoda RS, Geraghty B, Rennert H, Narula N and Fernandes HD: Accuracy of next-generation sequencing for the identification of clinically relevant variants in cytology smears in lung adenocarcinoma. *Cancer Cytopathol* 125: 398-406, 2017.
- Faber E, Grosu H, Sabir S, Lucas FAS, Barkoh BA, Bassett RL, Luthra R, Stewart J and Roy-Chowdhuri S: Adequacy of small biopsy and cytology specimens for comprehensive genomic profiling of patients with non-small-cell lung cancer to determine eligibility for immune checkpoint inhibitor and targeted therapy. *J Clin Pathol* 75: 612-619, 2022.
- Ramani NS, Chen H, Broaddus RR, Lazar AJ, Luthra R, Medeiros LJ, Patel KP, Rashid A, Routhort MJ, Stewart J, *et al.*: Utilization of cytology smears improves success rates of RNA-based next-generation sequencing gene fusion assays for clinically relevant predictive biomarkers. *Cancer Cytopathol* 129: 374-382, 2021.
- Pepe F, Pisapia P, Gristina V, Rocco D, Micheli M, Micheli P, Iaccarino A, Tufano R, Gragnano G, Russo G, *et al.*: Tumor mutational burden on cytological samples: A pilot study. *Cancer Cytopathol* 129: 460-467, 2021.
- Sanghvi RV, Buhay CJ, Powell BC, Tsai EA, Dorschner MO, Hong CS, Lebo MS, Sasson A, Hanna DS, McGee S, *et al.*: Characterizing reduced coverage regions through comparison of exome and genome sequencing data across 10 centers. *Genet Med* 20: 855-866, 2018.
- Wang Q, Shashikant CS, Jensen M, Altman NS and Girirajan S: Novel metrics to measure coverage in whole exome sequencing datasets reveal local and global non-uniformity. *Sci Rep* 7: 885, 2017.
- Chou D, Chen X, Purdy A, Teng L, Luo B, Zhao C, Ball L, Castaneda A, Clark K, Crain B, *et al.*: Abstract 3732: Analytical performance of TruSight® Tumor 170 on small nucleotide variations and gene amplifications using DNA from formalin-fixed, paraffin-embedded (FFPE) solid tumor samples. *Cancer Res* 2017.



Copyright © 2025 Loderer *et al.* This work is licensed under a Creative Commons Attribution-NonCommercial-NoDerivatives 4.0 International (CC BY-NC-ND 4.0) License.